

System Identification of Anti-Vibration Units in Semiconductor Exposure Apparatus

H. Kato*, S. Wakui*, T. Mayama*, A. Toukairin⁺, H. Takanashi⁺, and S. Adachi⁺

*CANON INC.

Design Dept.15

Semiconductor Production Equipment Development Center

20-2 Kiyohara-Kogyo-danchi, Utsunomiya

Tochigi, 321-3292, Japan

Phone : +81 28 667 5711

Fax : +81 28 670 5301

⁺Dept. Electrical, Electronic Eng.

Utsunomiya University

7-1-2 Yoto, Utsunomiya

Tochigi, 321-8585, Japan

Phone : +81 28 689 6125

Fax : +81 28 689 6125

Abstract

In this paper, system identification of semiconductor exposure apparatus is discussed. It has a multi-degrees-of-freedom mechanism which includes anti-vibration units for microvibration control. A dynamical model of the mechanism is necessary in order to design the microvibration controller. The model is practically constructed in a short time using subspace method. Identification results are evaluated through experimental data in comparison with conventional frequency response method.

1. Introduction

Vibration control is one of the fundamental technologies in semiconductor exposure apparatus. Disturbing vibration has to be reduced to meet nanometer semiconductor lithography demands for alignment accuracy. Anti-vibration units are mounted in semiconductor exposure apparatus for this purpose. These units prevent the transmission of external vibration to the exposure apparatus. Recently the "active anti-vibration unit" has been developed, which makes effective vibration control possible by driving its actuator according to the external vibration.

A dynamical model of the anti-vibration unit is necessary in order to design vibration control systems. Fundamental design procedure is based on one-degree-of-freedom (1DOF) motion model. However, the controlled object is essentially a multi-DOF mechanism because semiconductor exposure apparatus has multiple anti-vibration units. Therefore, the controlled object is treated as a multi-input-multi-output (MIMO) system to design the control system strictly and to evaluate the control performance. If the model is constructed from the physical laws, the precise mechanical parameters of the motional mechanism are necessary. The more DOF increases, the more complex the dynamical model becomes. It is desirable that the model is con-

structed using some experimental method independent of the precise information of the controlled object.

In order to evaluate the performance of the vibration control systems, the performance has to be explicitly presented by some method. Up to now, time response or frequency response is utilized, considering some single input and some single output of the MIMO system. This method needs long measurement time for all input-output combinations and is a hard task for production field. It is desirable to identify the performance of the MIMO system by other simpler methods.

Thus, the authors have derived the dynamical model of semiconductor exposure apparatus using the system identification theory [1], [2]. This paper describes the system identification of multi-DOF mechanism including anti-vibration units and its experimental data. Experimental reports concerning the system identification of MIMO system have been rarely presented in the field of vibration control, particularly experimental reports about the system identification of the multi-DOF mechanism in semiconductor exposure apparatus.

In this experiment, it is proposed that subspace method [3] is applied to the system identification of the multi-DOF mechanism. The reasons we use the subspace method are as follows. First, the subspace method is applicable to a MIMO system. Next, it is applicable whether or not the identification system includes closed-loops. In other words, the subspace method can be applied to both the open-loop and closed-loop models, the former is available for designing control systems and the latter presents control performance.

2. Semiconductor exposure apparatus

I-line or Krypton Fluoride (KrF) excimer laser lithography is used in mass production of DRAMs or microprocessor chip-layers. Semiconductor exposure apparatus

has the lithography system to expose circuit patterns on reticle to semiconductor wafer through projection lens. Fig.1 shows the overview of semiconductor exposure apparatus. The wafer is mounted on the micro-moving stage. The micro-moving stage compensates the tilt angular of the wafer and is mounted on the XY stage. The XY stage moves the wafer perpendicularly to the optical axis and enables continuous exposures to the wafer. This exposure system is mounted on the base plate. Several anti-vibration units support the base plate.

Fig.2 shows the front view of the structure of semiconductor exposure apparatus. Though only two anti-vibration units are shown in Fig.2, the exposure apparatus has actually two more units in its back. Four anti-vibration units support the exposure apparatus, and the

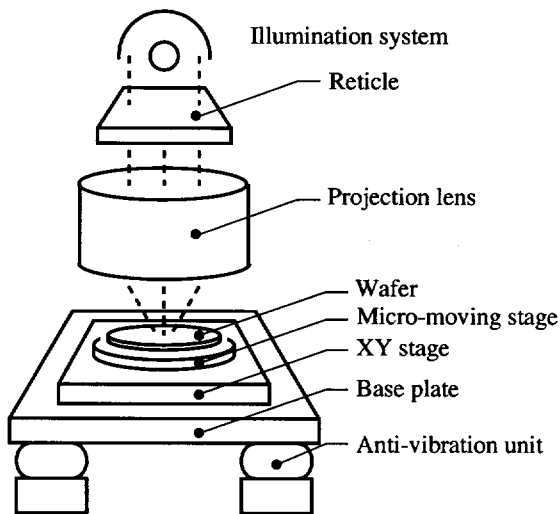


Fig.1 Overview of semiconductor exposure apparatus

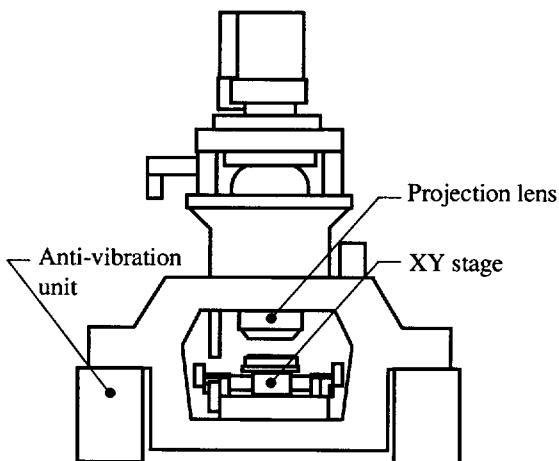


Fig.2 Structure of the exposure apparatus

units include actuators for absorbing or suppressing vibration of the exposure apparatus.

3. Anti-vibration units in semiconductor exposure apparatus

The anti-vibration unit in this experiment has air springs for supporting the exposure apparatus. Air springs easily generate enough force to support semiconductor exposure apparatus whose mass is over several thousand kilograms. Another advantage of air springs is that the position of the exposure apparatus is controllable by changing their internal air pressure.

Fig.3 shows the structure of the anti-vibration unit. Only vertical elements are drawn in Fig.3. The internal air pressure of the air spring is controlled by the air-valve which is an electric pressure transducer. The anti-vibration unit has the linear motor which is an actuator driving the exposure apparatus and the unit has the acceleration sensor detecting vibration of the exposure apparatus. The basic strategy of the vibration control by the anti-vibration unit is to support the exposure apparatus by the air spring as to isolate the apparatus from external vibration, and then to damp the vibration of the exposure apparatus by feeding back the vibration sensor signal to the linear motor or the air spring. The anti-vibration unit has also the horizontal sensor and the actuators, which are not drawn in Fig.3.

A dynamical model of the anti-vibration units is considered on condition that acceleration signals are not fed back. Dynamical characteristics of the anti-vibration units mainly depend on those of the air springs. In other words, the anti-vibration units can be regarded as stiff and viscous elements. Suppose the exposure apparatus supported by the anti-vibration units is a rigid body. Then the dynamical model is as shown in Fig.4 using a

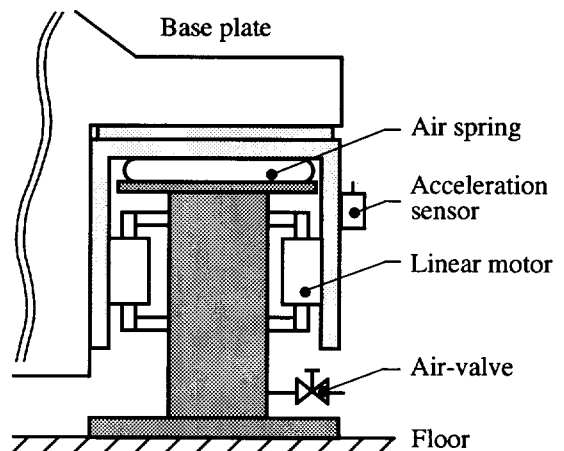


Fig.3 Vertical elements of the anti-vibration unit

rigid body with stiff and viscous elements. Since motion of a rigid body has 6DOF, the identification system is the motional mechanism with 6DOF, which is supported by stiff and viscous elements in its four corners. These elements are resolved into 3 components in the direction of $x, y,$ and z axes.

The equation of motion of the identification system is as follows. The origin of the rectangular coordinate system coincides with the center of gravity of the rigid body when the identification system is in equilibrium. Disturbance force \mathbf{F} acting on the rigid body is resolved into 6 components $F_x, F_y, F_z, M_x, M_y,$ and M_z as

$$\mathbf{F} = [F_x, F_y, F_z, M_x, M_y, M_z]^T, \quad (1)$$

where $F_x, F_y,$ and F_z are the translation forces and $M_x, M_y,$ and M_z are the moments. Displacement of the rigid body \mathbf{X} is also resolved into translations $x, y,$ and z and rotations $\theta_x, \theta_y,$ and θ_z as

$$\mathbf{X} = [x, y, z, \theta_x, \theta_y, \theta_z]^T. \quad (2)$$

Suppose the displacement \mathbf{X} and the velocity $\dot{\mathbf{X}}$ are small, and the $x, y,$ and z axes are the principal axes of inertia. Then, the equation of motion is described by

$$\mathbf{M}\ddot{\mathbf{X}} + \mathbf{C}\dot{\mathbf{X}} + \mathbf{K}\mathbf{X} = \mathbf{F}. \quad (3)$$

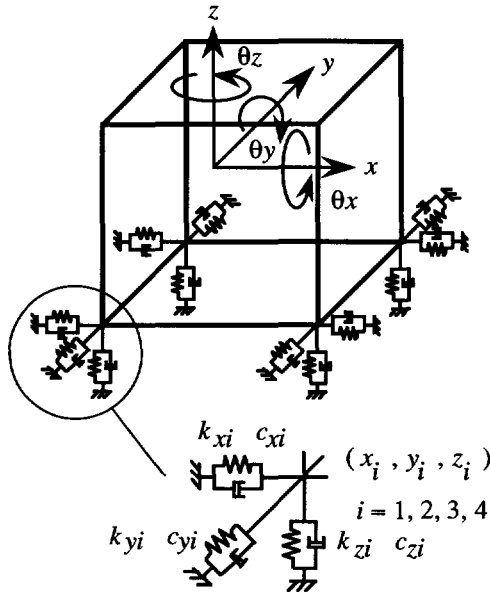


Fig.4 Dynamical model of the identification system

Inertia matrix \mathbf{M} is defined by

$$\mathbf{M} = \text{diag} [m, m, m, I_x, I_y, I_z]^T, \quad (4)$$

where m is the mass of the rigid body and $I_x, I_y,$ and I_z are the moments of inertia. \mathbf{C} is the 6×6 viscous matrix, given by

$$\mathbf{C} = \begin{bmatrix} c_{11} & 0 & 0 & 0 & c_{15} & c_{16} \\ 0 & c_{22} & 0 & c_{24} & 0 & c_{26} \\ 0 & 0 & c_{33} & c_{34} & c_{35} & 0 \\ 0 & c_{42} & c_{43} & c_{44} & c_{45} & c_{46} \\ c_{51} & 0 & c_{53} & c_{54} & c_{55} & c_{56} \\ c_{61} & c_{62} & 0 & c_{64} & c_{65} & c_{66} \end{bmatrix}, \quad (5)$$

where

$$\begin{aligned} c_{11} &= \sum c_{xi}, & c_{44} &= \sum (y_i^2 c_{zi} + z_i^2 c_{yi}), \\ c_{22} &= \sum c_{yi}, & c_{55} &= \sum (x_i^2 c_{zi} + z_i^2 c_{xi}), \\ c_{33} &= \sum c_{zi}, & c_{66} &= \sum (x_i^2 c_{yi} + y_i^2 c_{xi}), \\ c_{15} &= c_{51} = \sum z_i c_{xi}, & c_{16} &= c_{61} = -\sum y_i c_{xi}, \\ c_{24} &= c_{42} = -\sum z_i c_{yi}, & c_{26} &= c_{62} = \sum x_i c_{yi}, \\ c_{34} &= c_{43} = \sum y_i c_{zi}, & c_{35} &= c_{53} = -\sum x_i c_{zi}, \\ c_{45} &= c_{54} = -\sum x_i y_i c_{zi}, & c_{46} &= c_{64} = -\sum x_i z_i c_{yi}, \\ c_{56} &= c_{65} = -\sum y_i z_i c_{xi}, \end{aligned}$$

and $\sum_{i=1}^4 \mathbf{K}$ is the 6×6 stiffness matrix, given by

$$\mathbf{K} = \begin{bmatrix} k_{11} & 0 & 0 & 0 & k_{15} & k_{16} \\ 0 & k_{22} & 0 & k_{24} & 0 & k_{26} \\ 0 & 0 & k_{33} & k_{34} & k_{35} & 0 \\ 0 & k_{42} & k_{43} & k_{44} & k_{45} & k_{46} \\ k_{51} & 0 & k_{53} & k_{54} & k_{55} & k_{56} \\ k_{61} & k_{62} & 0 & k_{64} & k_{65} & k_{66} \end{bmatrix}, \quad (6)$$

where

$$\begin{aligned} k_{11} &= \sum k_{xi}, & k_{44} &= \sum (y_i^2 k_{zi} + z_i^2 k_{yi}), \\ k_{22} &= \sum k_{yi}, & k_{55} &= \sum (x_i^2 k_{zi} + z_i^2 k_{xi}), \\ k_{33} &= \sum k_{zi}, & k_{66} &= \sum (x_i^2 k_{yi} + y_i^2 k_{xi}), \\ k_{15} &= k_{51} = \sum z_i k_{xi}, & k_{16} &= k_{61} = -\sum y_i k_{xi}, \\ k_{24} &= k_{42} = -\sum z_i k_{yi}, & k_{26} &= k_{62} = \sum x_i k_{yi}, \\ k_{34} &= k_{43} = \sum y_i k_{zi}, & k_{35} &= k_{53} = -\sum x_i k_{zi}, \\ k_{45} &= k_{54} = -\sum x_i y_i k_{zi}, & k_{46} &= k_{64} = -\sum x_i z_i k_{yi}, \\ k_{56} &= k_{65} = -\sum y_i z_i k_{xi}. \end{aligned}$$

The input signals to the identification system are the disturbance forces to the exposure apparatus. In this

experiment, the linear motors, which are mounted in the anti-vibration units, are used as actuators driving the exposure apparatus. Let force commands to the linear motors be \mathbf{F} defined in Eq.(1). Force commands to the linear motors are not distinguished from the actual disturbance force acting on the exposure apparatus, because the linear motors generate driving forces which almost equal their input commands. In the discussion below, \mathbf{F} means both the force commands and the actual disturbance forces. The output signals are the accelerations of the exposure apparatus caused by the disturbance forces. Let the acceleration signals of the exposure apparatus be accelerations A_x, A_y , and A_z and angular accelerations $A_{\theta_x}, A_{\theta_y}$, and A_{θ_z} . They exactly coincide with $\ddot{\mathbf{X}}$ in Eq.(3).

The transfer function matrix \mathbf{G} from the input signals to the output signals is defined by

$$\begin{aligned} & [A_x, A_y, A_z, A_{\theta_x}, A_{\theta_y}, A_{\theta_z}]^T \\ & = \mathbf{G} [F_x, F_y, F_z, M_x, M_y, M_z]^T. \end{aligned} \quad (7)$$

The matrix \mathbf{G} is a 6×6 square matrix, having 36 elements of G_{ij} ($i, j = 1, 2, \dots, 6$) because the order of both input and output vector is 6. The purpose of this identification experiment is to identify the transfer function matrix \mathbf{G} . It is clear from the preceding discussion that the minimum order of the transfer function matrix \mathbf{G} is 12, since the dynamical model is the resonant system with 6DOF.

The force command \mathbf{F} described in motional mode $x, y, z, \theta_x, \theta_y$, and θ_z is converted into the force command to each linear motor by the motional mode operations. The accelerations are also calculated by the operations of the detecting signals of the acceleration sensors mounted in each anti-vibration unit. These motional mode operations are decided by the geometric assignment of both the anti-vibration units and the center of gravity of the exposure apparatus.

4. System identification experiments

In this section, system identification experiments are discussed. The input signals were six-uncorrelated PRBS (pseudo random binary signal). Period of the PRBS was 1023, clock frequency was 25 Hz. The input signals consisted of one period of the PRBS, thus experimental time was about 40 seconds. Six-uncorrelated input signals were simultaneously applied to the identification system so that all the motional mode should be excited. The input signals to the identification system and the output signals from the system were measured. Sampling frequency in the measurement was set to 1000 Hz. It is 40 times as large as the clock frequency of the PRBS.

Six-uncorrelated PRBS were generated by DSP (digital signal processor). These signals were converted into analog signals by the D/A converters. The linear motors were driven according to the signals through the motional mode operation circuit and the power amplifiers. Acceleration signals were generated from the detecting signals of the acceleration sensors through the motional mode operation circuit.

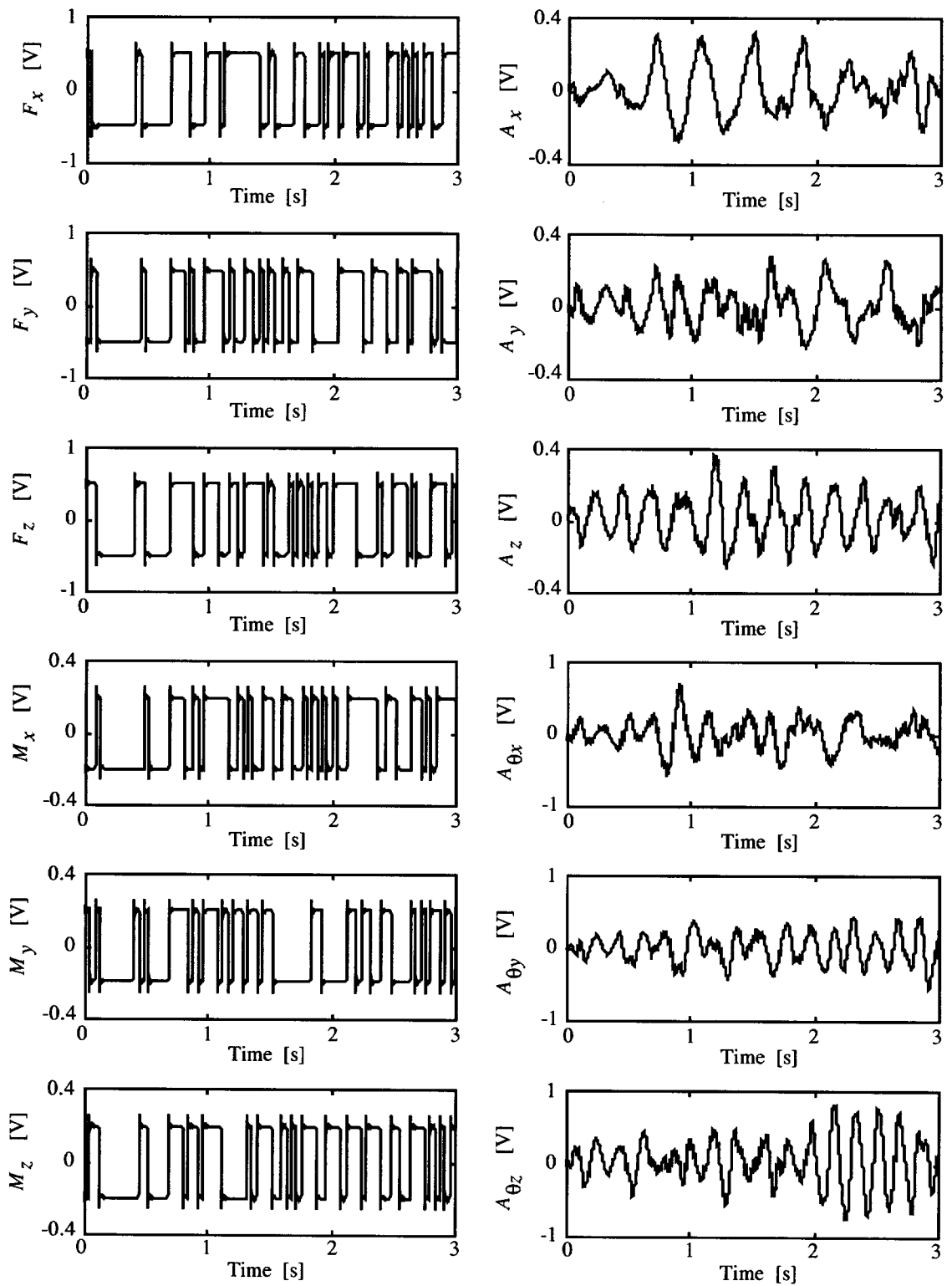
Fig.5 shows the input and the output signals. In this figure, (a) force commands and moment commands are the six-uncorrelated PRBS, and (b) accelerations are the output signals. Though time length of these signals is about 40 seconds, Fig.5 only shows the initial period of 3 seconds.

The sampling frequency for the measurement signal was converted into 100Hz by decimation technique. N4SID command in MATLAB System Identification Toolbox [4] was used for carrying out the subspace identification method. The order of the identification model was 18, which was decided considering that the minimum order of the identification system is 12 as described in the previous section and that there may exist time lags in the signal processing system.

The feedback gains were set so low as to ignore the effect of the vibration feedback control. Thus the dynamical characteristics of the controlled object can be identified. Identification results are evaluated in comparison with frequency transfer functions by conventional frequency response method, which was obtained using an FFT analyzer. Measurement time to obtain the one-input-one-output frequency transfer function was about 20 minutes in the frequency response method. It took 12 hours to measure all the 36 elements of the transfer function matrix \mathbf{G} defined in Eq.(7).

Fig.6 shows identification results in frequency domain. In this figure, solid line and dashed line stand for identification results by the subspace method and the frequency response method, respectively. It is clear that the resonant frequencies in the identification model coincide well with those in the frequency response method as shown in Fig.6. Since the resonant frequencies are previously known to be in this frequency domain, the model well identifies the resonant frequencies and the resonant magnitude. The vibration control systems including anti-vibration units are designed to compress these resonant peaks. Thus identification accuracy in this frequency domain is important.

On the contrary, there are a few differences between the identification model and the experimental results using the frequency response method in higher or lower frequency ranges particularly in Fig.6 (a) $G_{11} = A_x/F_x$ or



(a) Force commands and moment commands

(b) Accelerations

Fig.5 Input and output signals

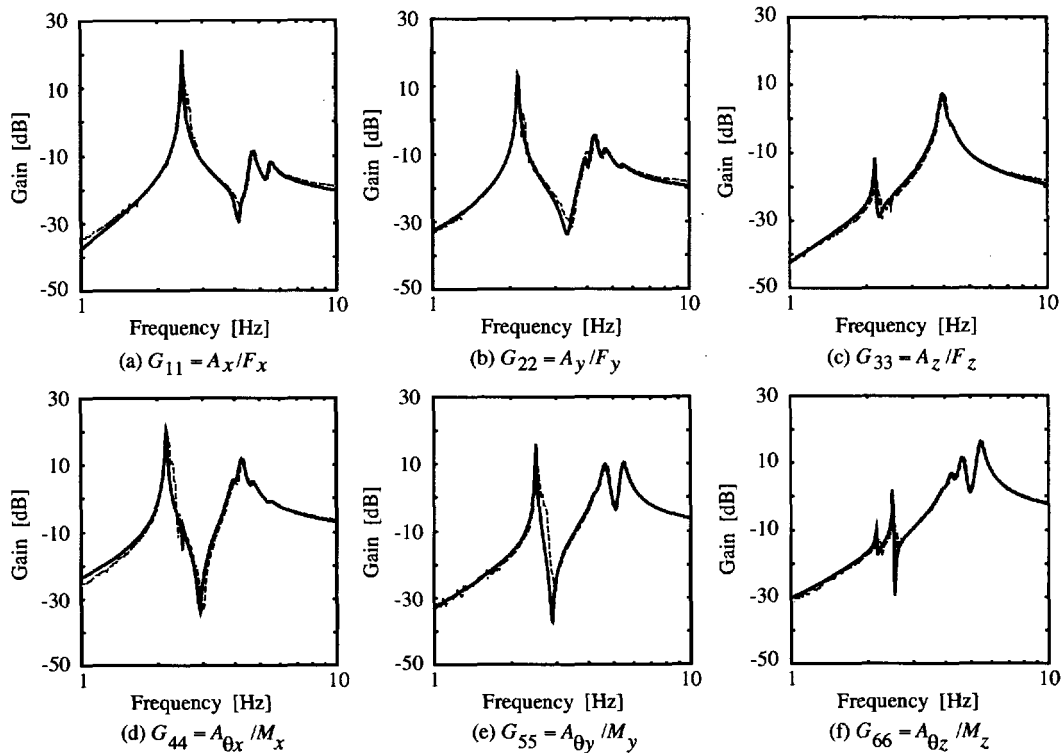


Fig.6 Identification results (Solid line : Subspace method, Dashed line : Frequency response method)

(b) $G_{44} = A_{\theta x}/M_x$. The accuracy of the identification model requires more precise evaluation in the future.

5. Conclusions

The findings of this paper are summarized as follows.

1. The dynamical model of the multi-DOF mechanism in semiconductor exposure apparatus is identified by using the subspace method.
2. All the motional DOF of the mechanism are simultaneously excited and the multi-DOF dynamical model is identified from the simultaneous exciting signals and the acceleration signals.
3. The identification model coincides well with the experimental results in the frequency response method especially in the resonant frequency domain.

The advantage of using the system identification theory is that the measurement time can be reduced in comparison with the frequency response method, and that the MIMO model is derived for the purpose of designing control systems and evaluating the performance. We will improve the accuracy of the identification model and utilize it in the advanced design of the vibration control. The physical parameters presenting the dynamical characteristics of the mechanism can be estimated from the identified model. It is also useful for

mechanical design.

The identification model was derived without feedback-loops in this experiment. We intend to identify the system with closed-loops in the future. It can be a technique for evaluating the control performance. Though the closed-loops have an effect on controlling the damping coefficients of the resonant system, it is hard to estimate the damping coefficients from the conventional frequency responses. The damping coefficients can be obtained directly from the identified model.

References

- [1] S.Adachi et al., Modeling of semiconductor exposure apparatus via system identification theory, SICE'98, pp.115-116, 1998 (in Japanese)
- [2] A.Toukairin et al., System identification of semiconductor exposure apparatus using M-sequence input signal, SICE'98, pp.495-496, 1998 (in Japanese)
- [3] Van Overschee, P. and B.De Moor, N4SID: Subspace algorithms for the identification of combined deterministic-stochastic system, Automatica, Vol.30, pp.75-93, 1994
- [4] The MATH WORKS Inc., System identification toolbox user's guide, 1995